Measurements and Correlations of Transition Reynolds Numbers on Sharp Slender Cones at High Speeds

S. R. PATE*
ARO Inc., Arnold Air Force Station, Tenn.

An experimental investigation of laminar boundary-layer transition on a sharp, 10° total angle, insulated cone at zero yaw was conducted in the AEDC-VKF 12-in. and 40-in. supersonic wind tunnels at freestream Mach numbers from 3 to 6. This research was directed toward defining the relationship between the aerodynamic noise disturbances and boundary-layer transition Reynolds numbers [$(Re_t)_\delta$] in high-speed wind tunnels and has extended previously published planar results to include axisymmetric models. A significant increase in $(Re_t)_\delta$ with increasing tunnel size (similar to the planar results) is shown to exist. Sharp cone transition Reynolds numbers from eleven facilities (12–54 in.) for freestream Mach numbers from 3 to 14 and a unit Reynolds number per inch range from 0.1×10^6 to 1.2×10^6 have been correlated using aerodynamic-noise-transition parameters. A quantitative correlation of the ratio between cone and planar $(Re_t)_\delta$ values has been developed which demonstrates a strong Mach number dependence and also indicates a variation with tunnel size and unit Reynolds number.

Nomenclature

b = model nose bluntness, in.
C_F = mean turbulent skin-friction coefficient (tunnel wall)
c = tunnel test section circumference, in.
c_1 = tunnel test section circumference of 12- × 12-in. tunnel (c_1 = 48 in.)
l = model axial length, in.
l_m = axial distance from tunnel throat to model nose, in.
l_r = axial distance from tunnel throat to wall boundary-layer rake, in.
M = Mach number
p = surface probe Pitot pressure, psia
p_c = cone surface static pressure, psia
p_0 = tunnel stilling chamber pressure, psia
p_0' = total pressure downstream of a normal shock wave at freestream conditions, psia
p_∞ = freestream static pressure, psia
$\tilde{p}$ = root-mean-square of pressure fluctuation, psia
q_∞ = freestream dynamic pressure, psia
$\dot{q}$ = heat-transfer rate, Btu/ft²-sec
$(Re_t)_\delta$ = transition Reynolds number (based on local conditions), $(Re_t)_\delta = (Re/\text{in.})_\delta x_t$
Re_δ or $(Re/\text{in.})_\delta$ = inviscid flow local surface unit Reynolds number per in., U_δ/ν_δ
Re_∞ or $(Re/\text{in.})_\infty$ = freestream Reynolds number per in., U_∞/ν_∞
T = static temperature, °R and/or °F
T_0 = tunnel stilling chamber total temperature, °R and/or °F
U = velocity, fps
x = surface distance measured from cone apex, in.
x_t = surface distance location of boundary-layer transition, in.
δ^* = boundary-layer displacement thickness (tunnel wall), in.
θ_c = cone half-angle, deg
μ = absolute viscosity, lb-sec/ft²
ν = kinematic viscosity, in-fps

Subscripts

aw = adiabatic wall
c = cone configuration
Planar = two-dimensional configuration, either hollow cylinder or flat plate
w = wall
δ = local inviscid flow properties
∞ = freestream

Presented as Paper 70-799 at the AIAA 3rd Fluid and Plasma Dynamics Conference, Los Angeles, Calif., June 29–July 1, 1970; submitted August 13, 1970; revision received January 29, 1971. This research was sponsored by the Arnold Engineering Development Center (AEDC), Air Force Systems Command (AFSC), under Contract F40600-71-C-002 with ARO Inc., Arnold Air Force Station.

* Supervisor, Aerodynamics Section, Hypervelocity Branch, Aerophysics Division, von Kármán Gas Dynamics Facility (VKF). Associate Fellow AIAA.

I. Introduction

FACILITY-GENERATED disturbances (primarily vorticity or "turbulence") present in subsonic and low supersonic ($M_\infty \lesssim 3$) wind tunnels have long been recognized to have a significant and adverse effect on boundary-layer stability and transition experiments.[1–4]

For Mach numbers above about three, the sound field (aerodynamic noise) which radiates from turbulent boundary layers on the wall of supersonic wind tunnels[3–9] is a major source of freestream disturbances. It was mentioned by Morkovin[4] and stated by Laufer[5] that for high freestream Mach numbers ($M_\infty \gtrsim 2.5$) the sound field that radiates from the turbulent boundary layer on the walls of supersonic tunnels is a major source of freestream disturbance and must be considered in all stability and transition experiments. For example, the intensity of radiated noise limited the supersonic stability experiments of Laufer and Vrebalovich[6] to a maximum Mach number of 2.2. Laufer continued has investigations of the pressure field radiated by a turbulent boundary layer and reported on the intensity, characteristics, and properties of aerodynamic noise in Refs. 5 and 7. However, the influence of aerodynamic noise on transition was not directly demonstrated in these earlier studies.[3–7] Consequently, it has been the policy of most transition investigators to assume that the disturbance modes present at high Mach numbers ($M_\infty \gtrsim 3$), primarily radiated sound or aerodynamic noise, had negligible effects on the location of transition and on the development of the transition process.

Recent experimental transition research by Pate and Schueler[8] has shown conclusively the severe, adverse effect that the aerodynamic noise which radiates from the turbulent boundary layer on the walls of supersonic and hypersonic

tunnels will have on transition. These studies have provided an extensive and unique aerodynamic noise-transition Reynolds number correlation of high-speed ($3 \leq M_\infty \leq 8$) wind-tunnel $(Re_t)_\delta$ data from many different facilities. The intensity of the radiated noise, as reported in Ref. 8, was related to the tunnel size, tunnel wall boundary-layer state (laminar, transitional, or turbulent) tunnel unit Reynolds number, and the tunnel Mach number.

Morkovin[9] has recently presented an exhaustive and thorough review on the state-of-the-art of transition and stability with critical comments included. Considerable attention was devoted to the influence of freestream disturbances at high Mach numbers. Included in Ref. 9 are experimental freestream disturbance measurements taken by Kendall in the JPL 20-in. supersonic wind tunnel with laminar and turbulent boundary layers on the tunnel walls. These results, taken at $M_\infty = 4.5$, showed a large difference in the spectra of freestream fluctuations when the boundary layer was laminar, as opposed to when turbulent flow existed on the tunnel walls.

Over the years, experimentalists have attempted to establish a valid relationship between cone and flat plate transition Reynolds numbers. Perhaps the most significant experimental results to date in this area were those reported in Refs. 10 and 11. From a qualitative comparison of $(Re_t)_\delta$ data obtained on axisymmetric and planar models from several sources and several different wind tunnels, Potter and Whitfield[10] observed that the $(Re_t)_\delta$ ratio (cone-to-planar) appeared to decrease from a value of approximately three at $M_\delta = 3$ to about one near $M_\delta = 8$. However, more recently Whitfield and Iannuzzi[11] concluded that attempts at direct comparison of cone and planar $(Re_t)_\delta$ data from various high-speed facilities must now be viewed with reservation and that cone-planar $(Re_t)_\delta$ ratio results cannot be clearly established from presently available experimental data. Their conclusions were based primarily on the recent transition studies of Plate and Schueler.[8] Therefore, evidence to date appears to indicate that the freestream disturbances present in high-speed test facilities are also masking the factor of three difference between cone and flat plate $(Re_t)_\delta$ values that have been reported experimentally and implied by many investigators using the semi-theoretical incompressible analysis of Tetervin.[12]

This research has extended the investigation of tunnel aerodynamic noise effects on transition to include axisymmetric models. Slender cone models have been tested at $3 \leq M_\infty \leq 6$ to determine if cone transition Reynolds numbers varied appreciably with the tunnel size and to establish if an aerodynamic noise-transition correlation similar to the planar results of Ref. 8 could be developed.

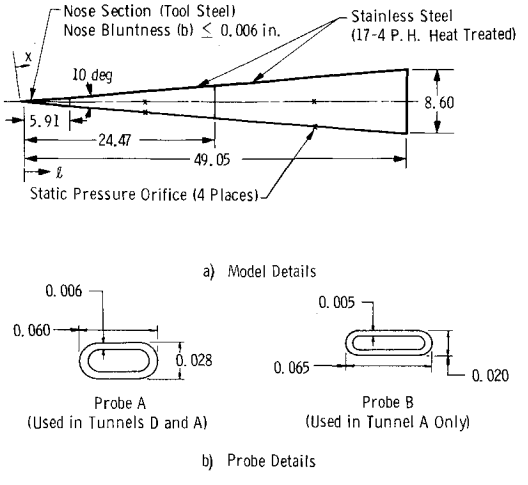

Fig. 1 Model geometry; all dimensions in inches; Tunnel D model configuration l = 24.47 in.; Tunnel A model configuration l = 49.05 in.; model surface finish 10–5 μin.

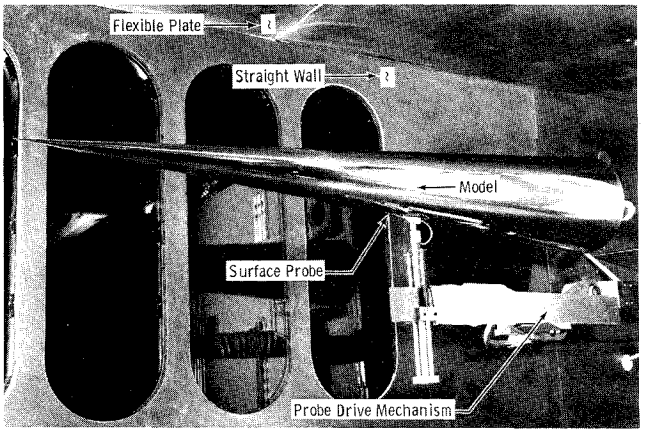

Fig. 2 Tunnel A cone model installation.

These transition studies have also provided new information on the relation between cone and flat plate (planar) transition Reynolds numbers, obtained in high-speed ($3 \leq M_\infty \leq 8$), conventional wind tunnels.

II. Experimental Conditions

Wind-Tunnel Facilities

New experimental data included in this report were obtained at the Arnold Engineering Development Center (AEDC) in the von Kármán Gas Dynamics Facility (VKF), Supersonic Tunnels A and D.

Tunnel D is an intermittent, variable-density wind tunnel with a manually adjusted, flexible plate-type nozzle and a 12- by 12-in. test section. The tunnel can be operated at Mach numbers from 1.5 to 5 at stagnation pressures from about 5 to 60 psia and at average stagnation temperatures of about 70°F.

Tunnel A is a continuous, closed-circuit, variable-density wind tunnel with an automatically driven, flexible plate-type nozzle and a 40- by 40-in. test section. The tunnel can be operated at Mach numbers from 1.5 to 6 at maximum stagnation temperatures up to 290°F ($M_\infty = 6$). Minimum operating pressures range from about one-tenth to one-twentieth of the maximum pressures.

Transition Models and Apparatus

The transition model, Figs. 1 and 2, was a 10° total angle, stainless steel cone equipped with a tool steel nose section. The model had a surface finish of approximately 10 μin. and a tip bluntness (b) between 0.005 and 0.006 in. The Tunnel D model consisted of the nose and center section, as shown in Fig. 1. The Tunnel A model was obtained by adding an aft section as shown in Figs. 1 and 2. In order to maintain a near perfect joint between the sections, the model surface was refinished after attaching each model section.

A remotely controlled, electrically driven, surface Pitot probe provided a continuous trace of the probe pressure on an X-Y plotter from which the location of transition was determined, Figs. 1 and 2.

Schlieren and shadowgraph photographic systems were used as a secondary method for detecting the location of transition in Tunnels D and A, respectively.

A $\frac{1}{4}$-in.-diam flush-mounted surface microphone having a frequency response from 0 to 30 kHz and a dynamic response from 70 to 180 db was also used to measure the model surface pressure fluctuations in the laminar, transitional, and turbulent flow regimes and to determine the location of transition.

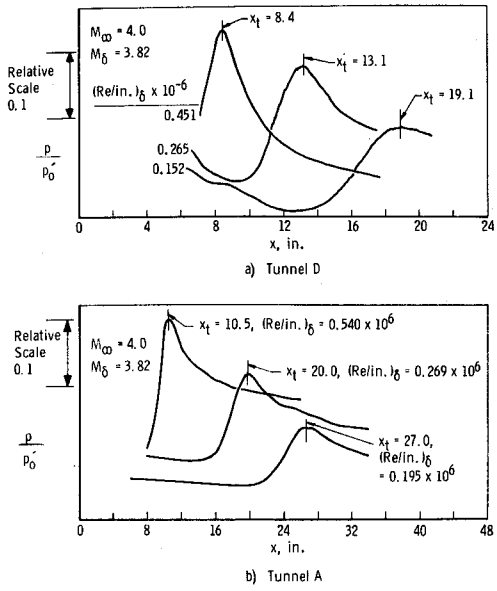

Fig. 3 Examples of surface probe transition profile traces.

III. Inviscid Flow Cone Properties

In reviewing published transition results it became apparent that inconsistencies existed in the calculation of tunnel unit Reynolds numbers and more often for cone surface values. These differences were traceable primarily to the different viscosity relationships used. Therefore, the surface Reynolds number ratios [Eq. (1)] assuming inviscid flow over sharp, unyawed cones were calculated using the linear [Eq. (2)] or Sutherland [Eq. (3)] viscosity law, depending on the value of the local flow static temperature:

$$(Re_\delta)_c/Re_\infty = (p_c/p_\infty)(M_c/M_\infty)[T_\infty/T_c]^{1/2}\mu_\infty/\mu_c \quad (1)$$

$$T \lesssim 215°\text{R}, (\mu)_{\text{linear}} = (0.0805 \times 10^{-8}) \times (T), \text{lb-sec/ft}^2 \quad (2)$$

$$T \gtrsim 216°\text{R}, \quad (\mu)_{\text{Southerland}} = \frac{2.270 \times (T)^{1.5}}{198.6 + T} \times 10^{-8}, \text{ lb-sec/ft}^2 \quad (3)$$

A combination of the viscosity laws allows the freestream viscosity to be determined using the linear law and the cone surface value evaluated using the Sutherland law, which is often the conditions existing in wind tunnels at high supersonic and hypersonic Mach numbers.

IV. Basic Transition Results

Methods of Detection

Surface probe

Typical surface probe transition profiles obtained in Tunnels D and A are presented in Fig. 3 for several unit Reynolds numbers. Unless otherwise specified, the location of transition used in this study is defined as the peak in the Pitot pressure profile, as illustrated in Fig. 3. This method of transition detection is generally accepted as being near the end of the transition region[13,14] and has been established as one of the more repeatable and reliable methods of selecting a particular and finite location of transition.

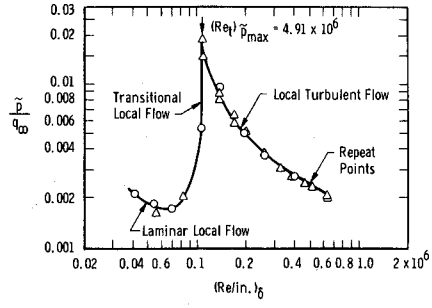

Fig. 4 Indication of transition from microphone root-mean-square pressure fluctuations, M_∞ = 3 (Tunnel A).

Microphone

Pressure fluctuation data obtained in Tunnel A with the flush mounted $\frac{1}{4}$-in.-diam surface microphone are shown in Fig. 4. The sharp apex in the pressure profile was defined as the indication of transition at the microphone location. The transition Reynolds number, based on this definition, will be compared with the Pitot probe values in subsequent figures. It is of interest to note the similarity between the root-mean-square (rms) profiles and other type measurements of the transition region, e.g., the surface probe (Fig. 3), heat-transfer rates[15,16] and heat-transfer fluctuations.[17] Additional information on the spectral distribution of the pressure fluctuations in the laminar, transitional, and turbulent boundary layers on this configuration and a description of the microphone instrumentation and recording procedures are reported in Ref. 18.

Photographic observations

The location of transition as determined from schlieren and shadowgraph photographs was selected at the body station where the boundary layer had developed into what appeared visually to be fully turbulent flow. This location of transition provided $(Re_t)_\delta$ values, in general, about 10–20% lower than $(Re_t)_\delta$ results obtained from the surface probe peak pressure locations. Any burst, ripples, or rope effects that were observable upstream of the fully developed turbulent location were ignored in the selection of x_t. The transition values pre-

Sym	Configuration	Surface Ray	Method of Detection	Source	ℓ_m, in.
△	5-deg Cone	Top	Schlieren	Present Study	44
○	5-deg Cone	Bottom	Schlieren	Present Study	44
□	5-deg Cone	Bottom	Surface Probe (p_{peak})	Present Study	44
----	Hollow Cylinder	Bottom	Surface Probe (p_{peak})	Refs. 8 and 13	48

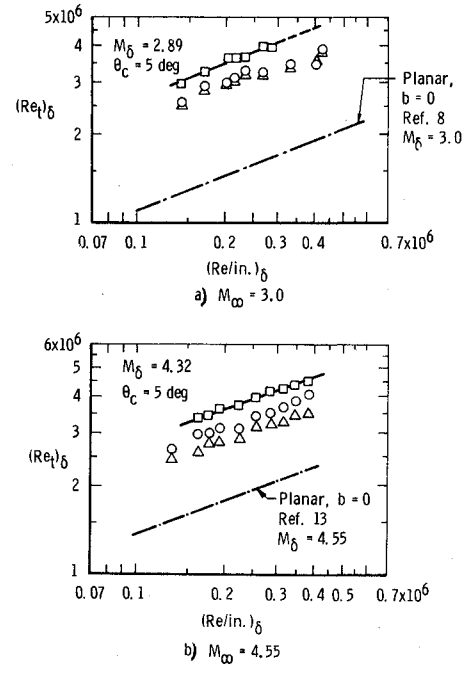

Fig. 5 Transition Reynolds number data from the AEDC-VKF 12- × 12-in. Tunnel D, sharp cone and planar models.

sented represent an average x_t value determined from approximately four different photographs.

Transition Reynolds Numbers

To maintain as nearly identical freestream flow disturbances as possible, the cone was positioned in the tunnel very near the previous hollow cylinder locations and the experiments were conducted at equivalent freestream Mach number and unit Reynolds number values.

The transition Reynolds number results for Tunnel D and A are presented in Figs. 5 and 6 and appear quite normal in that they exhibit the usual increase in $(Re_t)_\delta$ with increasing $(Re/\text{in.})_\delta$, and the photographic values are about 10–20% lower than the surface probe values. Although the microphone results were limited to two data points ($M_\infty = 3$ and 4), the peak in the pressure fluctuation profile appeared to provide $(Re_t)_\delta$ values consistent with the surface probe and photographic values.

One of the known (but sometimes forgotten) variables that can effect the transition location is the dew point or temperature at standard atmospheric pressure at which water condensation occurs.[19] In Tunnel D the dew point was sufficiently low (<0°F) at all Mach numbers not to affect the x_t locations. Also in Tunnel A† the dew point was sufficiently

Sym	Configuration	Surface Ray	Method of Detection	Source	ℓ_m, in.
△	5-deg Cone	Top	Shadowgraph	Present Study	215
○	5-deg Cone	Bottom	Shadowgraph	Present Study	215
□	5-deg Cone	Bottom	Surface Probe (p_{peak})	Present Study	215
---→	Hollow Cylinder	Side	Surface Probe (p_{peak})	Ref. 8	213, 231
×	5-deg Cone	Top	Microphone ($\tilde{p}_{max}$)	Present Study	215

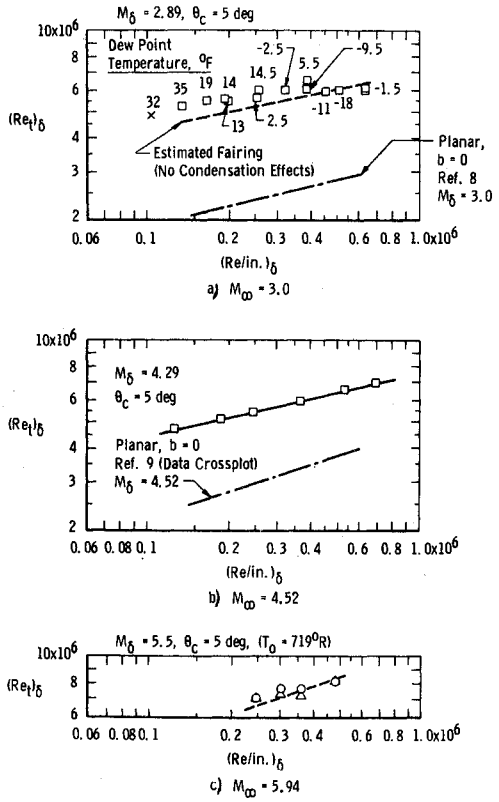

Fig. 6 Transition Reynolds number data from the AEDC-VKF 40- × 40-in. Tunnel A, sharp cone and planar models.

† The relatively high dew point existing in the $M_\infty = 3$ data reflect facility limitations existing on that particular date and does not necessarily represent standard test conditions.

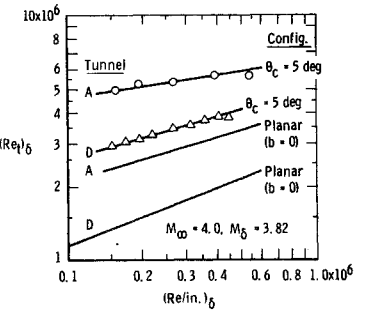

Fig. 7 Variation of transition Reynolds numbers with tunnel size.

low at all Mach numbers except for the lower unit Reynolds numbers (subatmospheric pressure levels) at $M_\infty = 3$, as illustrated in Fig. 6a. Therefore, a suggested $(Re_t)_\delta$ trend, as indicated by the dashed line, has been included in Fig. 6a for $M_\infty = 3$.

V. Transition Correlation

There was a large increase in the cone $(Re_t)_\delta$ values from Tunnels D and A at all test Mach numbers, as can be readily determined by a comparison of the data in Figs. 5 and 6.

Figure 7 presents a direct comparison of the $M_\infty = 4$ cone $(Re_t)_\delta$ data from Tunnels D and A. The large increase in $(Re_t)_\delta$ with increasing tunnel size is clearly evident and is very similar to the planar results from Ref. 8, which are included for a quantitative comparison. The increase in $(Re_t)_\delta$ with increasing tunnel size is explained by a decrease in the aerodynamic noise intensities that radiate from the turbulent boundary layer on the tunnel walls, as discussed in detail in Ref. 8.

Transition Reynolds numbers on the sharp slender cones were correlated, as shown in Fig. 8, using the aerodynamic-noise-transition parameters developed by Pate and Schueler.[8] A comprehensive discussion of the aerodynamic-noise-transition correlating parameters (δ^*, C_F, and c) is given in Ref. 8. Data used in the cone correlation were obtained not only from the present investigation, but also from a total of eleven sources representing eleven different wind tunnel facilities. The data covered a freestream Mach number range from 3 to 14, a $(Re/\text{in.})_\infty$ range from 0.1×10^6 to 1.2×10^6, and test section sizes from 12 in.[2] to 54 in. diam. Specific information on the range of test conditions and pertinent

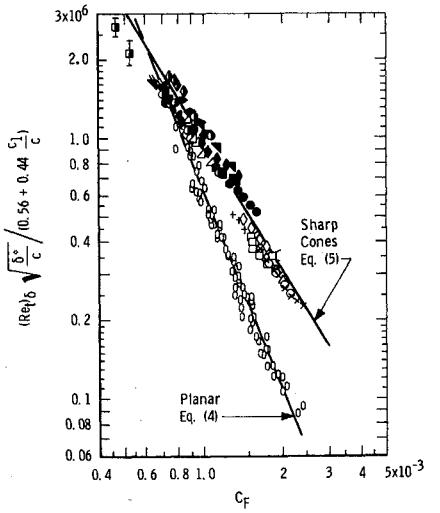

Fig. 8 Correlation of planar and sharp slender cone transition Reynolds numbers; Planar data and Eq. (4) from Ref. 8. Based on data from nine different wind-tunnel facilities varying in size from 1 to 16 ft, Mach number range from 3 to 8, and $(Re/\text{in.})_\infty$ range from 0.05×10^6 to 1.1×10^6. Symbol notation for cone data is consistent with Table 1.

Table 1 Source and range of data used in the transition Reynolds number correlations (Figs. 8 and 9)

Source	Sym	M_∞	M_δ	b x 10^3	θ_c, deg	$(Re/in.)_\infty$ x 10^{-6}	Tunnel	Test Section Size	Method of Transition Detection	*Amount of Adjustment	ℓ_m, in.	T_w/T_{aw}	T_w/T_0	Method of δ^* Determination
Present Study	○ △ □ ◇	3 3.5 4 4.55	2.9 3.4 3.8 4.3	5 (Sharp)	5	0.15 to 0.4	AEDC-VKF D	12 by 12 in.	Peak Probe Pressure	No Adjustment	44	≈1.0	0.90	Experimental Data ℓ_r = 56 in. Ref. 28
Present Study	● ■ ◆ ◥ ◀	3 4 4.5 5 5.9	2.9 3.8 4.3 4.7 5.5	5 (Sharp)	5	0.15 to 0.6	AEDC-VKF A	40 by 40 in.	Peak Probe Pressure Shadowgraph	No Adjustment	215	≈1.0	≈0.90	Experimental Data ℓ_r = 208 in. Refs. 8 and 29
Ref. 10 and VKF	◖** ◖** ◖	6 8 8	5.5 7.0 6.4	Sharp	6 6 9	0.16 to 0.43 0.16 to 0.29 0.12 to 0.29	AEDC-VKF B	50-in. Diam	Maximum $\dot{q}$ Maximum $\dot{q}$ Shadowgraph	1.08 No Adjustment No Adjustment	245	0.72 0.48 ≈0.93	0.63 0.41 ≈0.81	VKF Experimental Data and Ref. 30 ℓ_r = 244 in.
Ref. 33	◥**	10	8.5	Sharp	6	0.13	AEDC-VKF C	50-in. Diam	Maximum $\dot{q}$	No Adjustment	≈300	≈0.29	≈0.25	VKF Experimental Data, $\ell_r \approx$ 300 in.
VKF	◥	10	7.5	Sharp	9	0.17	AEDC-VKF C	50-in. Diam	Shadowgraph	1.1	≈300	≈0.77	≈0.66	
Ref. 11	◘**	14.2	9.3	4 (Sharp)	9	0.12, 0.2	AEDC-VKF F (Hotshot)	54-in. Diam	Maximum $\dot{q}$	No Adjustment	350	≈0.22	≈0.19	Ref. 32, ℓ_r = 384 in.
Ref. 10	◿** ◿**	6 8	5.0 6.2	Sharp	10 10	0.34 to 1.2 0.35 to 0.54	AEDC-VKF E	12 by 12 in.	Shadowgraph	1.1 1.1	≈64 ≈64	≈0.86 ≈0.6	≈0.75 ≈0.5	Estimated Using δ^* Correlation Ref. 8 ℓ_r = 64 in.
Ref. 34	◆**	10.2	9.2	4 to 10 (Sharp)	3.75	0.10 to 0.19	NASA-Langley	31 by 31 in. Hypersonic	Maximum $\dot{q}$	No Adjustment	158	0.43 to 0.63	0.37 to 0.54	ℓ_r = 158 in.
Ref. 15	X	3.1	3.0	<6 (Sharp)	5	0.1 to 0.67	NACA-Lewis	12 by 12 in.	Maximum T_w	1.19	≈40	≈1.0	≈0.90	ℓ_r = 47 in.
Ref. 16	+	5.0	4.9	3 (Sharp)	2.5	0.16 to 0.47	NASA-Lewis	12 by 12 in.	Maximum T_w	1.13	≈47	≈1.0	≈0.90	ℓ_r = 55 in.
Ref. 35	◻	3.84	3.67	<1 (Sharp)	5	0.18 to 0.46	JPL-SWT	9 by 12 in.	Maximum T_w	1.19	≈49	≈1.0	≈0.90	Experimental Data Ref. 31, ℓ_r = 49 in.
Ref. 40	◑	≈11.3	≈10.1	1 (Sharp)	5	0.04 to 0.16	GE Shock Tunnel	54-in. Diam (Nozzle Exit)	Maximum $\dot{q}$	No Adjustment	≈156	≈0.25	0.2	δ^* Correlation Ref. 32, ℓ_r = 156 in.

*Adjustment for Method of Detection Based on Refs. 13 and 14

**Cool-Wall Model

‡Nitrogen Test Gas

information on model geometry are provided in Table 1. Also included in Fig. 8 is the correlation of two-dimensional $(Re_t)_\delta$ data taken from Ref. 8. $(Re_t)_\delta$ data obtained with detection methods other than a surface probe were adjusted in accordance with the findings of Refs. 13 and 14, as specified in Table 1.

An empirical equation for the two-dimensional planar correlation was reported in Ref. 8 to be

$$[(Re_t)_\delta]_{\text{planar}} = [0.0141(C_F)^{-2.55}][0.56 + 0.44(c_1/c)]/[\delta^*/c]^{1/2} \quad (4)$$

An empirical equation that fits the cone data fairly well in Fig. 8 can be written as

$$[(Re_t)_\delta]_{\text{cone}} = 10.5(C_F)^{-1.66}[0.56 + 0.44(c_1/c)]/[\delta^*/c]^{1/2} \quad (5)$$

Although the sharp cone data in Fig. 8 correlated fairly well using the planar correlating parameters from Ref. 8, the correlation exhibits two systematic inconsistencies. First, the slope of a linear fairing of the data [Eq. (5)] is somewhat steeper than the slopes of most of the individual data sets. Second, the data from the larger tunnels show a systematic grouping somewhat higher than the smaller tunnels. Systematic differences of this type and magnitude were not apparent in the correlation of the planar data.

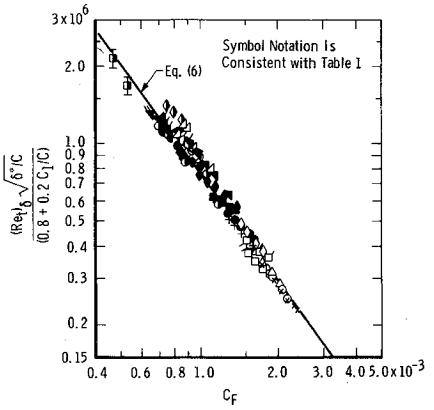

Fig. 9 Correlation of sharp slender cone transition Reynolds numbers.

These two inconsistencies have been eliminated by establishing a different normalizing parameter which accounts for tunnel size. Using the procedure described in Ref. 8, the tunnel size normalizing parameter for sharp slender cone $(Re_t)_\delta$ data was determined to be $(0.8 + 0.2c_1/c)$.

Presented in Fig. 9 is the correlation of the $(Re_t)_\delta$ data using the slender cone normalizing parameter. A significantly improved correlation of the data was accomplished. An empirical equation that represents a linear fairing of the data is provided by Eq. (6):

$$[(Re_t)_\delta]_{\text{cone}} = 48.5(C_F)^{-1.40}[0.8 + 0.2(c_1/c)]/[\delta^*/c]^{1/2} \quad (6)$$

Equation (4–6) are not statistical fits and represent the best visual linear fit of the data.

One factor that must be recognized in the correlation of cone data is the absence of a one-to-one relation or even a constant ratio between the freestream and cone surface unit Reynolds numbers. If a series of cone angles had been selected that would have allowed a constant ratio of certain cone to freestream parameters—say the unit Reynolds number ratio—to have been maintained, then any relationship that might have existed between the strength of the cone bow shock wave and the influence of the radiated noise levels on the cone laminar flow after passage through the bow shock might possibly have remained more constant. Future investigations in these areas would, of course, be desirable.

Since the correlation only included $(Re_t)_\delta$ from sharp slender cones ($\theta_c \leq 10°$), caution should be exercised when using the correlation to predict transition location on large angle cones with a strong bow shock wave.

Table 2 Transition data used for comparing Mach number and tunnel size (Fig. 10)

Sym	M_∞	Configuration	Facility	Source	Method of Detection**
■	3, 4, 5	Hollow Cylinder, b = 0	AEDC-VKF-D (12 by 12 in.)	Ref. 8	Peak Probe Pressure (No Adjustment)
♦	5, 6.1, 7.1, 8	Flat Plate, b = 0	AEDC-VKF-E (12 by 12 in.)	Ref. 8	Peak Probe Pressure (No Adjustment)
◥	3.7, 4.6	Flat Plate, b = 0	JPL-SWT (18 by 20 in.)	Ref. 8	Maximum Surface Shear (No Adjustment)
●	3, 4, 5	Hollow Cylinder, b = 0	AEDC-VKF-A (40 by 40 in.)	Ref. 8	Peak Probe Pressure (No Adjustment)
▲	6, 8	Hollow Cylinder and Flat Plate, b = 0	AEDC-VKF-B (50-in. Diam)	Ref. 8	Peak Probe Pressure (No Adjustment)
* ◆	3	Hollow Cylinder	AEDC-PWT-16S (16 by 16 ft)	Ref. 8	Peak Probe Pressure (No Adjustment)
□	3, 3.5, 4, 4.5	Sharp Cone, θ_c = 5 deg	AEDC-VKF-D (12 by 12 in.)	Present Study	Peak Probe Pressure (No Adjustment)
○	3, 4, 4.5, 5, 5.9	Sharp Cone, θ_c = 5 deg	AEDC-VKF-A (40 by 40 in.)	Present Study	Peak Probe Pressure (M_∞ = 5.9, Shadowgraph) (No Adjustment)
* ◇	6.1, 8	Sharp Cone, θ_c = 10 deg	AEDC-VKF-E (12 by 12 in.)	Ref. 10	Shadowgraph (Adjusted by Factor of 1.1)**
○	3.1, 3.8	Sharp Cone, θ_c = 7.5 deg	R.A.E. (5 by 5 in.)	Ref. 36	Shadowgraph (No Adjustment)
▽	10.2	Sharp Cone, θ_c = 3.75 deg	NASA Langley (31 by 31 in.)	Ref. 34	Maximum $\dot{q}$ ($0.4 \leq (T_W/T_0) \leq 0.63$) (No Adjustment)
▷	10	Sharp Cone, θ_c = 5 deg	R.A.C. (36-in. Diam)	Ref. 37	Maximum $\dot{q}$ ($0.075 \leq (T_W/T_0) \leq 0.36$) (No Adjustment)
◁	10	Sharp Cone, θ_c = 6 deg	AEDC-VKF-C (50-in. Diam)	Ref. 33	Maximum $\dot{q}$ ($(T_W/T_0) = 0.25$) (No Adjustment)
△	8	Sharp Cone, θ_c = 9 deg	AEDC-VKF-B (50-in. Diam)	VKF and Ref. 10	Shadowgraph ($(T_W/T_0) \approx 0.8$, Hot Wall) (No Adjustment)
△	6	Sharp Cone, θ_c = 6 deg	AEDC-VKF-B (50-in. Diam)	VKF and Ref. 10	Maximum $\dot{q}$ ($(T_W/T_0) \approx 0.63$) (Adjusted by Factor of 1.08)**
◁	10	Sharp Cone, θ_c = 9 deg	AEDC-VKF-C (50-in. Diam)	VKF	Shadowgraph ($(T_W/T_0) \approx 0.66$, Hot Wall) (Adjusted by Factor of 1.1)**
◨	14.2 ± 0.3	Sharp Cone, θ_c = 9 deg	AEDC-VKF-F (54-in. Diam)	Ref. 11	Maximum $\dot{q}$ ($(T_W/T_0) \approx 0.19$) (No Adjustment)
+	≈11.3	Sharp Cone, θ_c = 5 deg	GE Shock Tunnel (54-in. Diam)	Ref. 40	Maximum $\dot{q}$ ($(T_W/T_0 \approx 0.2$) (No Adjustment)

*Extrapolated Data
**Amount of Adjustment Based on Results of Present Study and Refs. 10, 13, and 14

The average turbulent skin-friction coefficients (C_F) used in the transition correlation were determined using Ref. 20 in conjunction with the tunnel freestream Mach number and a length Reynolds number based on $(Re/\text{in.})_\infty$ and the model axial location (l_m) as measured from the tunnel throat. Information concerning the determination of the tunnel wall δ^* values is provided in Table 1.

There are several significant results (other than the basic correlation which was independent of Mach number and unit Reynolds number) to be deduced from Figs. 8 and 9.

1) The data correlations and the basic $(Re_t)_\delta$ data have established that—at least in conventional supersonic and hypersonic wind tunnels—radiated noise is a major and dominating influence on the transition location and process. The significantly different logarithmic slopes exhibited by the aerodynamic-noise-transition correlations of the cone and planar $(Re_t)_\delta$ data suggest that aerodynamic noise disturbances influence the transition process on sharp slender cones differently than on planar bodies.

2) The sharp cone and planar correlations in Fig. 8 appear to intersect at the low C_F values ($M_\infty \gtrsim 8$) and diverge as C_F increases ($M_\infty \to 3$). This trend implies that the ratio of cone to planar $(Re_t)_\delta$ values is dependent on Mach number, tunnel size, and unit Reynolds number. A detailed discussion on this subject will be persued in Sec. VII.

3) A literal interpretation of the correlation suggests that in Tunnel F, planar $(Re_t)_\delta$ values would be larger than cone values. The validity of this inference will have to wait for experimental verification.

The reader should be aware that the $(Re_t)_\delta$ correlations presented in Figs. 8 and 9 are applicable only to wind tunnels having turbulent wall boundary layers. Consequently, the correlations cannot be used for evaluation of ballistic range or free-flight transition locations. Furthermore, the experimental data and correlations presented should not be used to reach conclusive decisions regarding the "true" Mach number and unit Reynolds number variations that might exist in a disturbance-free environment (either free-flight or experiment facility).

VI. Tunnel Size and Mach Number Effects

A composite plot of data from the present study and several other sources is presented in Fig. 10. The data included in Fig. 10 are identified in Table 2. These results firmly establish the existence of a significant increase in cone and planar $(Re_t)_\delta$ values with increasing tunnel size. The data presented also clearly indicate that only by comparing data obtained in identical test environments can a valid and meaningful relationship between cone and planar $(Re_t)_\delta$ ratios be established.

Figure 10 also adds substantial support to the conclusion of Ref. 8 that the "true" Mach number effect on transition cannot be established from wind-tunnel models exposed to aerodynamic noise. It is perhaps also of interest to note the difference in Mach number trends between the cone and planar $(Re_t)_\delta$ data which exists even when the fairing is based on data from similar size tunnels.

The predicted $(Re_t)_\delta$ values obtained using Eqs. (4–6) are also included in this figure and the agreement with the experimental data in both trends and levels is considered quite satisfactory. Equation (6) is seen to provide better agreement with the cone data than does Eq. (5). Based on the results of Figs. 8 and 9, this is as expected.

Variations of transition with tunnel size is perhaps most strikingly demonstrated at $M_\infty = 3$, where the cone and planar data were obtained in tunnels varying in size from 5- to 40-in. and 1- to 16-ft, respectively.

Concerning Mach number effects, the reader is referred to the results obtained by Stainback at NASA-Langley,[21] which were represented and discussed in Ref. 8. These studies report that when the tunnel and cone local unit Reynolds number were held approximately constant and the cone local Mach number was varied from about 4 to 8—by proper selection of cone angles—then the $(Re_t)_\delta$ values were independent

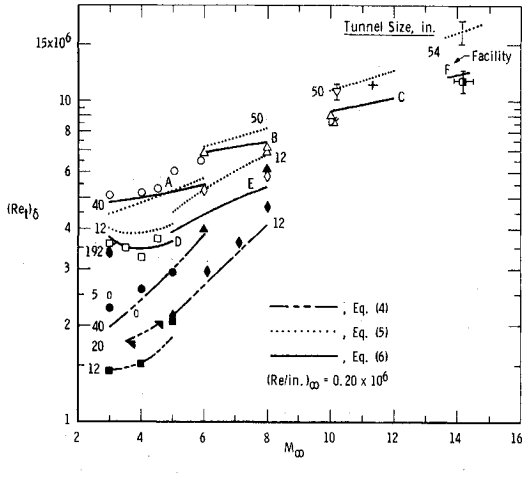

Fig. 10 Variation of axisymmetric and planar transition Reynolds numbers with tunnel size and Mach number.

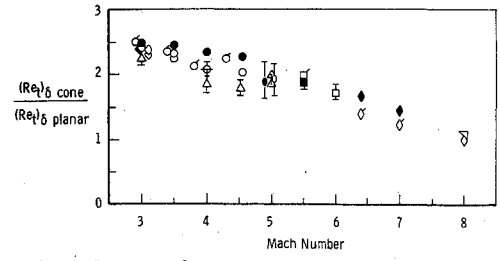

Fig. 11 Correlation of axisymmetric and planar transition Reynolds number ratios. Flagged symbols—evaluated at equivalent $(Re/in.)_\delta$ and M_δ values $(Re/in.)_\delta = 0.2 \times 10^6$; open symbols—evaluated at equivalent $(Re/in.)_\delta$ and M_∞ values; solid symbols—evaluated at equivalent $(Re/in.)_\infty$ and M_δ values (from data cross plots).

of Mach number. These results are in agreement with the proposed aerodynamic-noise-transition relation and with the correlations presented in Figs. 8 and 9.

VII. Axisymmetric and Planar Transition Correlation

Based on the results of Ref. 8, it was realized that a correlation was possible only if cone and flat plate data were obtained in the same test facility, under identical test conditions, and using equivalent methods of transition detection. Consequently, it was necessary to obtain $(Re_t)_\delta$ data exposed to various intensity levels of radiated noise while continuing to maintain a constant freestream unit Reynolds number and Mach number if the cone-planar $(Re_t)_\delta$ relation was to be determined. This was accomplished by obtaining test data in significantly different size tunnels (AEDC-VKF Tunnels A and D).

Presented in Fig. 11 is a correlation of cone and flat plate $(Re_t)_\delta$ data developed from the data obtained in this study and Ref. 8 (VKF Tunnels A and D) and data from three other test facilities. Table 3 provides detailed information on the data presented in Fig. 11. Based on the results of Ref. 8, it can be argued that there are various procedures that are available for reducing this type data. The three procedures used are outlined in the legend of Fig. 11. The significant conclusions to be drawn from this figure are 1) the $(Re_t)_\delta$ ratio appears to be about 2.2–2.5 at $M_\infty = 3$; 2) the trend decreases monotonically with increasing Mach number to a value of approximately 1.0–1.1 at $M_\infty = 8$; 3) close inspection of these results at a given Mach number ($M_\infty = 3$–5) suggests a decrease in the $(Re_t)_\delta$ ratio with increasing tunnel size (this finding is in agreement with the correlation results presented in Fig. 8); and 4) the $(Re_t)_\delta$ ratio is also slightly dependent on the method of analysis.

An empirical equation for the cone-planar $(Re_t)_\delta$ ratios can be obtained by ratioing Eqs. (4) and (5) or (4) and (6).

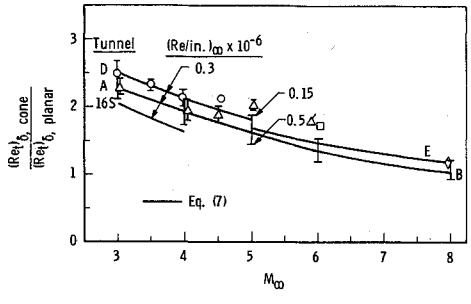

Fig. 12 Comparison of predicted and measured cone-planar transition ratios.

Table 3 Data used in correlation of axisymmetric and planar $(Re_t)_\delta$ ratios (Fig. 11)

Sym	Config.	θ_c, deg	M_∞	M_δ	$(Re/in.)_\delta \times 10^{-6}$	Facility	Method-of-Detection	Source
○	Sharp Cone	5	3 to 4.5	2.9 to 4.3	0.15 to 0.4	VKF-D (12 by 12 in.)	Peak Pitot Pressure	Present Study
	Hollow Cylinder (b = 0)	-	3 to 4.5	3 to 4.5				Refs. 8 & 13
△	Sharp Cone	5	3 to 5	2.9 to 4.7	0.15 to 0.6	VKF-A (40 by 40 in.)	Peak Pitot Pressure	Present Study
	Hollow Cylinder (b = 0)	-	3 to 5	3 to 5				Ref. 8
□	Sharp Cone	5, 6	6	5.5	0.15 to 0.4	VKF-A VKF-B (50-in. Diam)	Shadowgraph $\dot{q}_{maximum}$	Present Study VKF
	Flat Plate (b ≈ 0)	-	6	6			Peak Pitot Pressure	Refs. 8 & 38
◇	Sharp Cone	6, 9	8	7.0, 6.4	0.2, 0.3	VKF-B (50-in. Diam)	$\dot{q}_{max}$ and Shadowgraph	Refs. 10 & VKF
	Hollow Cylinder (b = 0)	-	8	8			$(T_w)_{max}$, Peak Pitot Pressure	Ref. 14
▽	Sharp Cone	6, 9	8	7.0, 6.4	0.2	VKF-B (50-in. Diam)	$\dot{q}_{max}$ and Shadowgraph	Ref. 10 & VKF
	Flat Plate (b ≈ 0)	-	8	8			Peak Pitot Pressure	Ref. 39
◇	Sharp Cone	5	3.1	2.98	0.1 to 0.6	NACA (12 by 12 in.)	T_w max	Ref. 15
	Hollow Cylinder	-	3.1	3.1				
○	Sharp Cone	2.5	5.0	4.90	0.15 to 0.5	NASA (12 by 12 in.)	T_w max	Ref. 16
	Hollow Cylinder	-	5.0	5.0				

The equation obtained by ratioing Eqs. (4) and (6) is presented to illustrate the results obtained:

$$\frac{(Re_t)_{\delta,\text{cone}}}{(Re_t)_{\delta,\text{planar}}} = \frac{\text{Equation (6)}}{\text{Equation (4)}} = 3440(C_F)^{1.15}\left[\frac{0.8 + 0.2(c_1/c)}{0.56 + 0.44(c_1/c)}\right] \quad (7)$$

Predicted transition ratios using Eq. (7) are presented in Fig. 12 for a large range of tunnel sizes, Mach numbers, and $(Re/in.)_\infty$ values. The experimental data for the 12-, 40-, and 50-in. tunnels ($3 \leq M_\infty \leq 8$) are in good agreement with the empirically predicted ratios. The data also indicate, qualitatively at least, a decrease in the transition ratio with an increase in tunnel size. The data included in Fig. 12 are identified in Table 4.

Table 4 Data used in cone-planar transition ratios (Fig. 12); experimental data evaluated at equivalent $(Re/in.)_\infty$ and M_∞ values

Sym	Config.	θ_c, deg	M_∞	M_δ	$(Re/in.)_\infty \times 10^{-6}$	Facility	Method of x_t Detection	Source
○	Sharp Cone	5	3 to 4.5	2.9 to 4.3	0.15 to 0.5	VKF-D (12 by 12 in.)	Peak Surface Pitot Probe Pressure	Present Study
	Hollow Cylinder (b = 0)	-	3 to 4.5	3 to 4.5	0.15 to 0.5			Refs. 8 & 13
△	Sharp Cone	5	3 to 5	2.9 to 4.7	0.15 to 0.5	VKF-A (40 by 40 in.)	Peak Surface Pitot Probe Pressure	Present Study
	Hollow Cylinder (b = 0)	-	3 to 5	3 to 5	0.15 to 0.5			Ref. 8
◁	Sharp Cone	5	5.9	5.5	0.2	VKF-A (40 by 40 in.)	Schlieren	Present Study
	Hollow Cylinder (b = 0)	-	5.9	5.9	0.2		Schlieren	Data Extrapolation from Ref. 8
□	Sharp Cone	6	6	5.5	0.2	VKF-B (50-in. Diam)	Max Heat Trans. (Adjusted by 1.08)	Ref. 10 & VKF
	Flat Plate (b = 0)	-	6	6	0.2		Peak Pitot Pressure	Refs. 8 & 38
◇	Sharp Cone	6, 9	8	7.0, 6.4	0.15 to 0.3	VKF-B (50-in. Diam)	Max Heat Trans.	Ref. 10 & VKF
	Hollow Cylinder (b = 0)	-	8	8	0.15 to 0.3		Peak Pitot Pressure	Ref. 14

Many investigators of transition have referenced the theoretical results of Battin and Lin[22] and Tetervin[12] when attempting to explain the experimental values of cone-planar transition Reynolds number ratios.

Battin and Lin[22] concluded that the minimum critical Reynolds number ($R_{x,\,cr}$) for a cone was three times larger than for a flat plate. However, the agreement between the ratio of approximately three exhibited by previously published transition data at moderate supersonic Mach numbers and the stability theory ratio of three (although an interesting observation) is perhaps only fortuitous as demonstrated by the data correlations presented in Figs. 11 and 12.

Tetervin[12] also used the linear theory of incompressible boundary-layer stability and obtained an approximate relation for a Reynolds number ratio between cones and flat plates which varied between one and three.

It can be stated that these experimental results, in general, support the conclusions of Tetervin[12] in that the cone-planar transition Reynolds number does not have a constant value of three but can vary between one and three. The validity of the linear-theoretical model proposed by Tetervin[12] is, however, not established by the experimental data presented in this paper.

VIII. Comparison of Tunnel and Range Results

Figure 13 presents a direct and quantitative comparison of transition data from sharp slender cones obtained in wind tunnels and an aeroballistic range[23] at equivalent local Mach numbers using similar methods of detection. At a comparable $(Re/\text{in.})_\delta$ value, these data suggest that the range $(Re_t)_\delta$ data are significantly lower than the tunnel results, even for the 12-in. tunnel.

A recent publication by Sheetz[24] has shown that the unit Reynolds number effect is also present in sharp cone $(Re_t)_\delta$ data obtained in the NOL Ballistic Range at $M_\infty = 7.5$.

One major nonsimilarity between the tunnel and range experimental conditions is in the surface temperature ratios. Transition reversals have been predicted theoretically[25] and verified experimentally[26, 27] for smooth bodies. However, to the author's knowledge, there are no experimental data that show transition Reynolds number to decrease below the adiabatic wall value for any degree of surface cooling for truly smooth bodies. Therefore, if comparisons could be made where the model wall to freestream temperature ratios were comparable, then a larger difference between tunnel and range $(Re_t)_\delta$ data than suggested by Fig. 13 might exist.

One question that naturally arises is whether adverse environmental or model disturbances could be affecting the range results. Only additional experimental range data can answer this question. The significance of the unit Reynolds number effect evident in the range data has been discussed in Refs. 23 and 24, and the results of preliminary investigations on range noise disturbances have been reported in Ref. 23.

IX. Concluding Remarks

The significant results obtained from this experimental research were the following.

1) Boundary-layer transition measurements made on a sharp, 10° total-angle cone in 12-in. and 40-in. wind tunnels at Mach numbers 3–4.5 have shown a significant increase in transition Reynolds numbers $(Re_t)_\delta$ with increasing tunnel size. The variation of $(Re_t)_\delta$ with tunnel size is explained by the aerodynamic noise which radiates from the tunnel wall turbulent boundary layer. These variations with tunnel size are in agreement with previously published planar results and provide additional confirmation of the severe adverse effect which radiated aerodynamic noise has on transition.

2) A correlation was developed of transition Reynolds number $(Re_t)_\delta$ data on sharp, slender cones from eleven different wind tunnel facilities covering a Mach number range from 3 to 14, a unit Reynolds number per inch range from 0.1×10^6 to 1.2×10^6, and tunnel test section sizes from 12 in. square to 54 in. diam. The correlation was independent of Mach number and unit Reynolds number and dependent only on the aerodynamic noise parameters established by Pate and Schueler for planar $(Re_t)_\delta$ data.

Sym	Facility	M_δ	T_w/T_{aw}	θ_c, deg	Source	Method of Detection
○	VKF Range K	4.3	≈ 0.18	10	Ref. 23	Shadowgraph - Schlieren
△	VKF Tunnel D (12 by 12 in.)	4.3	≈ 1.0	5	Present Study	Schlieren
□	VKF Tunnel A (40 by 40 in.)	4.3	≈ 1.0	5	Present Study	Surface Probe Peak Pressure Value Adjusted to Schlieren Location $(Re_t)_{schlieren} \approx 0.82\,(Re_t)_{p_{peak}}$
----	PWT Tunnel 16S (16 by 16 ft)	4.3	≈ 1.0	5	Present Study	Estimated Using $(Re_t)_\delta$ Correlation

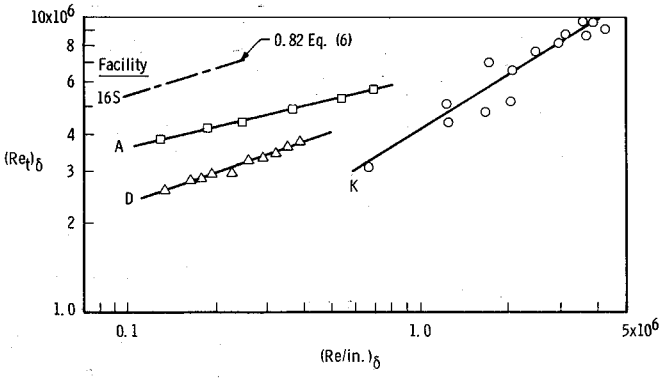

Fig. 13 Comparison of sharp cone transition Reynolds numbers from wind tunnels and an aeroballistic range.

3) These axisymmetric $(Re_t)_\delta$ data and the resulting aerodynamic-noise-transition correlation provide additional confirmation of the dominating influence that radiated aerodynamic noise can have on the transition process. These results also provide explicit support to the earlier suggestions by Pate and Schueler that extreme caution must be exercised when attempting to establish so-called "true" Mach number and unit Reynolds number trends from transition data obtained in conventional supersonic and hypersonic tunnels because of the strong adverse effect of aerodynamic noise disturbances.

4) The axisymmetric and planar aerodynamic-noise-transition correlations presented are applicable only to wind tunnels having turbulent wall boundary layers. The correlations presented cannot be used for the evaluation or prediction of ballistic range or atmospheric flight transition locations.

5) A quantitative correlation of cone-to-planar transition Reynolds number ratios was developed. The data correlation and an empirical equation (based on the aerodynamic-noise-transition correlation) show a monotonic decrease in the transition ratios with increasing Mach number over the range from 3 to 8. A dependence on tunnel size and unit Reynolds number, in addition to the Mach number trend, is also indicated.

6) Wind-tunnel $(Re_t)_\delta$ results are shown to be significantly higher than ballistic range data at $M_\delta = 4.3$ and $(Re/\text{in.})_\delta \approx 0.6 \times 10^6$.

References

[1] Schubauer, G. B. and Skramstad, H. K., "Laminar Boundary-Layer Oscillations and Transition on a Flat Plate," Rept. 909, 1948, NACA.

[2] Van Driest, E. R. and Boison, J. C., "Experiments on

Boundary-Layer Transition at Supersonic Speeds," *Journal of the Aeronautical Sciences*, Dec. 1957, pp. 885–899.

[3] Kovasnzy, L. S. G., "Turbulence in Supersonic Flow," *Journal of the Aeronautical Sciences*, Vol. 20, No. 10, 1953.

[4] Morkovin, M. V., "On Supersonic Wind Tunnels with Low Free-Stream Disturbances," *Journal of Applied Mechanics*, Paper 59-APM-10, Vol. 26, 1959, pp. 319–324.

[5] Laufer, J., "Aerodynamic Noise in Supersonic Wind Tunnels," *Journal of the Aerospace Sciences*, Vol. 28, 1961, pp. 685–692.

[6] Laufer, J. and Vrebalovich, T., "Stability and Transition of a Supersonic Laminar Boundary Layer on an Insulated Flat Plate," *Journal of Fluid Mechanics*, Vol. 9, Oct. 1960, pp. 257–299.

[7] Laufer, J., "Some Statistical Properties of the Pressure Field Radiated by a Turbulent Boundary Layer," *The Physics of Fluids*, Vol. 7, No. 8, 1964.

[8] Pate, S. R. and Schuler, C. J., "Effects of Radiated Aerodynamic Noise on Model Boundary Layer Transition in Supersonic and Hypersonic Wind Tunnels," *AIAA Journal*, Vol. 7, No. 3, March 1969, pp. 450–457; also AEDC-TR-67-236 (AD666644), March 1968, Arnold Engineering Development Center, Arnold Air Force Station, Tenn.

[9] Morkovin, M. V., "Critical Evaluation of Transition from Laminar to Turbulent Shear Layers with Emphasis on Hypersonically Traveling Bodies," TR-68-149, Air Force Flight Dynamics Lab., Wright-Patterson Air Force Base, Ohio.

[10] Potter, J. L. and Whitfield, J. D., "Boundary Layer Transition under Hypersonic Conditions," AGARDograph 97, Part III, AGARD Specialists' Meeting on Recent Developments in Boundary Layer Research, May 1965; also AEDC-TR-65-99 (AD462716), 1965, Arnold Engineering Development Center, Arnold Air Force Station, Tenn.

[11] Whitfield, J. D. and Iannuzzi, F. A., "Experiments on Roughness Effects on Boundary Layer Transition up to Mach 16," *AIAA Journal*, Vol. 7, No. 3, March 1969, pp. 465–470.

[12] Tetervin, N., "A Discussion of Cone and Flat-Plate Reynolds Numbers for Equal Ratios of the Laminar Shear to the Shear Caused by Small Velocity Fluctuations in a Laminar Boundary Layer," TN 4078, Aug. 1957, NACA.

[13] Potter, J. L. and Whitfield, J. D., "Effects of Unit Reynolds Number, Nose Bluntness and Roughness on Boundary Layer Transition," AEDC-TR-60-5 (AD234478), 1960, Arnold Engineering Development Center, Arnold Air Force Station, Tenn.

[14] Whitfield, J. D. and Potter, J. L., "The Influence of Slight Leading Edge Bluntness on Boundary Layer Transition at a Mach Number of Eight," AEDC-TDR-64-18 (ADA431533), 1964, Arnold Engineering Development Center, Arnold Air Force Station, Tenn.

[15] Brinich, P. F. and Sands, N., "Effect of Bluntness on Transition for a Cone and a Hollow Cylinder at Mach 3.1," TN 3979, 1957, NACA.

[16] Brinich, P. F., "Recovery Temperature, Transition, and Heat Transfer Measurements at Mach 5," TN D-1047, 1961, NASA.

[17] Owen, F. K., "Transition Experiments on a Flat Plate at Subsonic and Supersonic Speeds," AIAA Paper 69-9, New York, 1969.

[18] Pate, S. R. and Brown, M. D., "Acoustic Measurements in Supersonic Transitional Boundary Layers," ISA Paper 1.3.1, presented at the 15th National Instrument Society of American (ISA), Aerospace Symposium, May 5–7, 1969, Las Vegas, Nev.; also AEDC-TR-69-182 (AD694071), Oct. 1969, Arnold Engineering Development Center, Arnold Air Force Station, Tenn.

[19] Laufer, J. and Marte, J. E., "Results and a Critical Discussion of Transition Reynolds Number Measurements on Insulated Cones and Flat Plates in Supersonic Wind Tunnels," Rept. 20-96, 1955, Jet Propulsion Lab., Pasadena, Calif.

[20] Van Driest, E. R., "Turbulent Boundary Layer in Compressible Fluids," *Journal of the Aeronautical Sciences*, Vol. 18, No. 3, March 1951, pp. 145–160.

[21] Stainback, C. P., "Some Effects of Roughness and Variable Entropy on Transition at a Mach Number of 8," AIAA Paper 67-132, New York, 1967.

[22] Battin, R. H. and Lin, C. C., "On the Stability of the Boundary Layer over a Cone," *Journal of the Aeronautical Sciences*, Vol. 17, No. 7, July 1950, pp. 453–454.

[23] Potter, J. L., "Observations on the Influence of Ambient Pressure on Boundary Layer Transition," *AIAA Journal*, Vol. 6, No. 10, Oct. 1968, pp. 1907–1911.

[24] Sheetz, N. W., Jr., "Ballistics Range Experiments on the Effect of Unit Reynolds Number on Boundary-Layer Transition," *Proceedings of the 8th Navy Symposium on Aeroballistics*, Paper 7, Vol. 2, Naval Weapons Center, Corona, Calif., June 1969, pp. 201–215.

[25] Reshotko, E., "Transition Reversal and Tollmien-Schlichting Instability," *The Physics of Fluids*, Vol. 6, No. 3, 1963, pp. 335–342.

[26] Wisniewski, R. J. and Jack, J. R., "Recent Studies on the Effect of Cooling on Boundary Layer Transition at Mach 4," *Journal of Aerospace Sciences*, Vol. 28, No. 25, 1961.

[27] Richards, B. E. and Stollery, J. L., "Further Experiments on Transition Reversal at Hypersonic Speeds," *AIAA Journal*, Vol. 4, No. 12, Dec. 1966, pp. 2224–2226.

[28] Bell, D. R., "Boundary Layer Characteristics at Mach Number 2 through 5 in the Test Section of the 12-inch Supersonic Tunnel D," AEDC-TDR-63-192 (AD418711), Sept. 1963, Arnold Engineering Development Center, Arnold Air Force Station, Tenn.

[29] Jones, J., "An Investigation of the Boundary Layer Characteristics in the Test Section of a 40- by 40-inch Supersonic Tunnel," AEDC-TN-60-189 (AD245362), Oct. 1960, Arnold Engineering Development Center, Arnold Air Force Station, Tenn.

[30] Sivells, J. C. and Payne, R. G., "A Method of Calculating Turbulent Boundary Layer Growth at Hypersonic Mach Numbers," AEDC-TR-59-3 (AD208774), March 1959, Arnold Engineering Development Center, Arnold Air Force Station, Tenn.

[31] Dayman, B., Jr., "Comparison of Calculated with Measured Boundary Layer Thicknesses on the Curved Walls of the JPL 20-in. Supersonic Wind Tunnel Two-Dimensional Nozzle," TR 32-349, March 1963, Jet Propulsion Lab., Pasadena, Calif.

[32] Edenfield, E. E., "Contoured Nozzle Design and Evaluation for Hotshot Wind Tunnels," AIAA Paper 68-369, San Francisco, Calif., 1968.

[33] McCauley, W. D., Saydah, A. R., and Bueche, J. F., "Effect of Spherical Roughness on Hypersonic Boundary Layer Transition," *AIAA Journal*, Vol. 4, No. 12, Dec. 1966, pp. 2142–2148.

[34] Everhart, P. E. and Hamilton, H. H., "Experimental Investigation of Boundary Layer Transition on a Cooled 7.5-deg. Total-Angle Cone at Mach 10," TN D-4188, Oct. 1967, NASA.

[35] Van Driest, E. R. and McCauley, W. D., "The Effect of Controlled Three-Dimensional Roughness on Boundary Layer Transition at Supersonic Speeds," *Journal of the Aerospace Sciences*, Vol. 4, 1960, pp. 261–271.

[36] Rogers, R. H., "Boundary Layer Development in Supersonic Shear Flow," Rept. 269, April 1960, AGARD, NATO, Paris.

[37] Sanator, R. J. and DeCarlo, J. P., "Hypersonic Boundary Layer Transition Data for a Cold Wall Slender Cone," *AIAA Journal*, Vol. 3, No. 4, April 1965, pp. 758–760.

[38] Nagel, A. L., Savage, R. T., and Wanner, R., "Investigation of Boundary Layer Transition in Hypersonic Flow at Angle of Attack," TR-66-122, 1966, Air Force Flight Dynamics Lab., Wright-Patterson Air Force Base, Ohio.

[39] Deem, R. E. and Murphy, J. S., "Flat Plate Boundary Layer Transition at Hypersonic Speeds," AIAA Paper 65-128, New York, 1965.

[40] Softley, E. J. and Graber, B. C., "Experimental Observation of Transition of the Hypersonic Boundary Layer," *AIAA Journal*, Vol. 7, No. 2, Feb. 1969, pp. 257–263.